Dynamic Evaluation of LCL-type Grid-Connected Inverters with Different Current Feedback Control Schemes

Han, Yang; Li, Zipeng; Guerrero, Josep M.

Published in:
Proceedings of the 2015 9th International Conference on Power Electronics and ECCE Asia (ICPE-ECCE Asia)

DOI (link to publication from Publisher):
10.1109/ICPE.2015.7167816

Publication date:
2015

Document Version
Early version, also known as pre-print

Dynamic Evaluation of LCL-type Grid-Connected Inverters with Different Current Feedback Control Schemes

Yang Han[1,2], *Member, IEEE,* Zipeng Li[1,2], Josep M. Guerrero[3], *Fellow, IEEE*
[1] School of Mechatronics Engineering, University of Electronic Science and Technology of China, Chengdu 611731, China
[2] State Key Laboratory of Power Transmission Equipment & System Security and New Technology, Chongqing University, Chongqing 400044, China
E-mail: hanyang@uestc.edu.cn
[3] Department of Energy Technology, Aalborg University, 9220 Aalborg, Denmark

***Abstract*-- Proportional-resonant (PR) compensator and *LCL* filter becomes a better choice in grid-connected inverter system with high performance and low costs. However, the resonance phenomenon caused by *LCL* filter affect the system stability significantly. In this paper, the stability problem of three typical current feedback control schemes in *LCL* grid-connected system are analyzed and compared systematically. Analysis in s-domain take the effect of the digital computation and modulation delay into account. The stability analysis is presented by root locus in the discrete domain, the optimal values of the controller and filter with different feedback configurations are provided. The impacts of digital delay, PR parameters and *LCL* parameters on different control strategies are also investigated. Finally, the theoretical analysis are validated by simulation results.**

***Index Terms*-- grid-connected converter, active damping, dual-loop, current control.**

I. INTRODUCTION

Grid-connected inverter plays an important role in interconnecting renewable energy and the utility grid. High order *LCL* filter can attenuate harmonics produced by PWM inverter effectively with low cost and size [1]. However, the resonance peak produced by *LCL* filter can affect the stability of the system seriously. In order to stabilize the system, damping resistors can be added in series with capacitors or inductors to attenuate the resonance peak. But it brings power loss and decreases system efficiency [2]. The active damping methods are effective and flexible in stabilizing the system and has been widely used [3]. However, it's more complex and costly than passive damping methods.

The proportional resonant (PR) controller have been proved to be a good choice and applied to the single-phase grid-connected inverter system [4], [5]. The ideal PR controller can provide infinite gain at the resonate frequency. Therefore, the static error at the fundamental frequency can be totally eliminated. In recent literatures, the control and stability issues of the *LCL*-type grid-connected inverter have been extensively discussed [6] ,[7]. In [7], a pole placements method is proposed to assure system stability and dynamic response considering the impacts of PR, *LCL* parameters and digital delay by analyzing the root locus. But in [7], only one current feedback control scheme is analyzed, and the conclusion is drawn without considering the delay effect, thus it's not accurate when the digital controller is employed.

The single-loop current control applied in *LCL*-type grid-connected inverter can operate with good performance by utilizing the inherent damping effect introduced by the *LCL* inverter side current [8], [9]. This kind of control scheme is simple and effective, but the quality of the output current is not satisfactory [10]. Besides, the resonance can be suppressed by employing the multiloop control strategies [11]. The typical dual-loop control strategies includes converter current plus grid current (i_L plus i_g) feedback control scheme and capacitor current plus grid current (i_c plus i_g) feedback control scheme, these two kinds of control schemes provide similar dynamic performance [12] . However, the stability and dynamic performance between them has not been investigated yet.

In this paper, the discrete root locus of different delay time, PR controller and *LCL*-filter parameters with three different current feedback configurations are presented. The conclusion can be drawn that the i_L plus i_g and i_c plus i_g feedback control have the similar dynamic performance. When the system delay time increases, the stability of the i_L plus i_g and i_c plus i_g feedback system increases until the delay time is greater than the critical value (2.5 T_s), and the system stability decrease dramatically. Whereas, the system stability margin under the i_L feedback control decrease monotonically when T_d increases. From the stability analysis based on the root locus in discrete domain, the stability region of the delay time, PR and *LCL*-filter parameters can be obtained. The effect of delay time, PR and *LCL* filter parameters on the system stability has been obtained, and the optimal value for different control strategies are presented and compared. The conclusion contributes optimizing the design of *LCL* filter and PR controller parameters.

This work is supported by National Natural Science Foundation of China (NSFC) under grant No.51307015 and by Visiting Scholarship of State Key Laboratory of Power Transmission Equipment & System Security and New Technology (Chongqing University) (2007DA10512713405), and by Visiting Scholarship of China Scholarship Council (CSC), and the Oversea Academic Training Funds (OATF), UESTC.

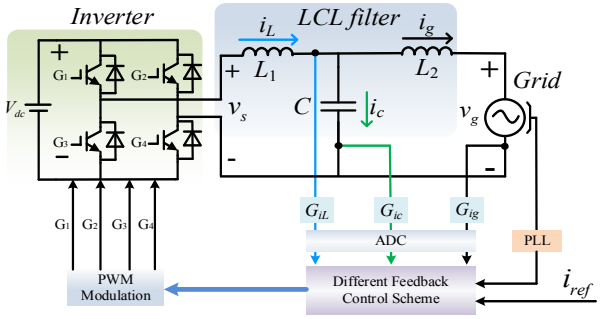

Fig. 1. Single-phase *LCL*-filter grid-connected inverter with current feedback control schemes.

II. System Modeling and Parameters Design

The topology of single-phase *LCL*-type grid-connected inverter system is shows in Fig. 1. A single-phase full-bridge voltage source inverter connected to the grid through an *LCL*-filter. The i_{ref} tracks the phase of the grid voltage based on the phase locked loop (PLL). The grid current i_g is regulated by the outer-loop controller $G_{PR}(s)$, and k_L is the proportional regulator in the inner-loop. G_{iL}, G_{ic} and G_{ig} represents the inverter-side current feedback factor, the capacitor current feedback factor and the grid-side current feedback factor, respectively. Fig. 2 shows the corresponding *s*-domain block diagrams of three typical current feedback control schemes.

The PR controllers are one of the linear controllers having resonant gain and can achieve zero steady-state at resonant frequency. Referring to [13], the transfer function in s-domain can be written as

$$G_{PR}(s) = k_p\left(1+\frac{2k_r\xi\omega_0 s}{s^2+2\xi\omega_0 s+\omega_0^2}\right) \tag{1}$$

With ω_0 being the resonant frequency, k_p being the proportional gain, k_r being the resonant gain, and ζ being the damping factor.

The transfer function describing the capacitor current i_c, converter current i_L and gird current i_g as a function of the converter output voltage v_s can be written as

$$G_{i_c/v_s}(s) = \frac{sCL_2}{s^2CL_1L_2+(L_1+L_2)} \tag{2}$$

$$G_{i_L/v_s}(s) = \frac{s^2L_2C+1}{s^3CL_1L_2+s(L_1+L_2)} \tag{3}$$

$$G_{i_g/v_s}(s) = \frac{1}{s^3CL_1L_2+s(L_1+L_2)} \tag{4}$$

The delay time from the control signals to drive signals can be expressed as $G_d(s) = e^{-sTd}$, and the Laplace transform of the delay time can be approximated by a rational transfer function using second order *pade* approximation with good accuracy [14], and the transfer function can be written as

$$G_d(s) = e^{-sT_d} \approx \frac{1-\frac{1}{2}sT_d+\frac{1}{12}s^2T_d^2}{1+\frac{1}{2}sT_d+\frac{1}{12}s^2T_d^2} \tag{5}$$

In order to analyze the system performance in s-domain, the corresponding open loop transfer function of the three feedback control schemes are derived, as shown in Fig. 2 .

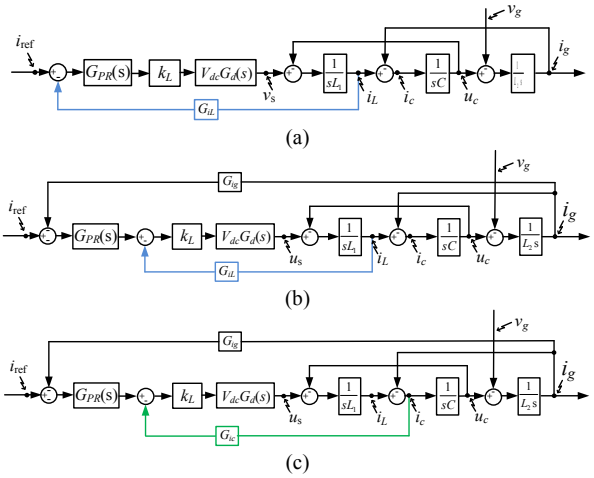

Fig. 2. The s-domain block diagrams of the inverters. (a) i_L feedback control. (b) i_L plus i_g feedback control. (c) i_c plus i_g feedback control.

TABLE I
Parameters of The Converter

Symbol	Values
V_{dc}	210 V
V_g	110√2 V
T_s	50 μs
T_d	50 μs
ω_0	100π rad/s
L_1	1500 μH
C	10 μH
L_2	1500 μH
K_I /K_p /K_r	0.08/0.5/50
ζ	0.01

A. The i_L feedback control scheme.

As can be seen in Fig. 2(a), the inverter current i_L feedback loop can be considered as the term on the forward path. And the open loop transfer function can be written as

$$G_a(s)_{open} = \frac{G_{PR}(s)k_LG_d(s)V_{dc}G_{i_g/v_s}(s)}{1+G_{PR}(s)k_LG_d(s)V_{dc}G_{i_L/v_s}(s)G_{iL}} \tag{6}$$

Using the parameters listed in Table I, the Bode diagrams of the open loop transfer functions $G_a(s)_{open}$ is shown in Fig. 3 (a), it's noticeable that the inverter current feedback control has the largest crossover frequency 1.72 kHz. But there is an obvious resonate peak near f_c which can be suppressed by adding passive damping resistors.

B. The i_L plus i_g feedback control scheme.

The open loop transfer function is

$$G_b(s)_{open} = \frac{G_{PR}(s)k_LG_d(s)V_{dc}G_{i_g/v_s}(s)}{1+k_LG_d(s)V_{dc}G_{i_L/v_s}(s)G_{iL}} \tag{7}$$

The Bode diagrams of the open loop transfer functions $G_b(s)_{open}$ is shown in Fig. 3 (b). It's obvious that the PR compensator provides a larger gain at f_0 than PI compensator thus the system performance is improved, but PR compensator also introduces negative phase shift at the resonate frequency which reduces the PM of the system.

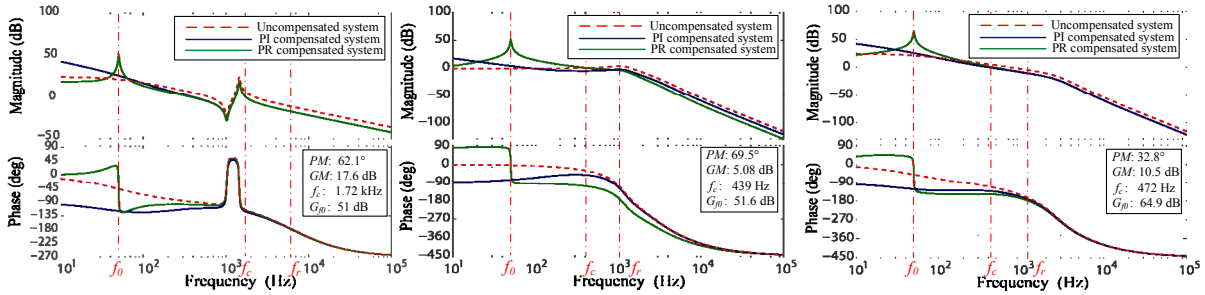

(a) (b) (c)

Fig.3. Bode diagrams of three open loop transfer functions (a) The i_L feedback control. (b) The i_L plus i_g feedback control. (c) The i_c plus i_g feedback control

C. *The i_c plus i_g feedback control scheme.*

The open loop transfer function is

$$G_c(s)_{open} = \frac{i_g(s)}{i_{ref}(s)} = \frac{G_{PR}(s)k_L G_d(s)V_{dc}G_{i_g/v_s}(s)}{1+k_L G_d(s)V_{dc}G_{i_c/v_s}(s)G_{ic}} \qquad (8)$$

The Bode diagrams of $G_c(s)_{open}$ is shown in Fig. 3 (c). It can be seen that the i_c plus i_g and i_L plus i_g feedback control provide better resonance damping effects over single i_L feedback control, while the PM of i_c plus i_g feedback system is relatively low.

To conclude, by employing the abovementioned current control schemes, the good dynamic performance and enough stability margin (with GM ≥ 5 dB and PM ≥ 45°) can be obtained. So they are all practical solution and can be analyzed through aforementioned s-domain models. When applying the single current feedback control scheme, the cost and the complexity is low, the system stability can be guaranteed if the system parameters are fixed or the passive method is used. Adding an extra current feedback can actively damp the resonance but the cost is also increased.

In the next section, the models are established in *z*-domain, the root locus of the discrete model are presented to analyze the system performance and the stability margin with different system parameters.

III. Discrete-Domain Modeling And Analysis

With the development of the digital controllers, the price/performance ratio of digital signal processor (DSP) is decreasing dramatically. Many control strategies for digitally controlled grid-connected inverter have been proposed [1], [15] without considering the inherent discrete sampling and the effect of control delay [16]. Therefore, the modeling for those novel digitally controlled system in *s*-domain is not accurate in all frequency range.

Fig. 4 shows the *z*-domain modeling of the digital control schemes. By using the Tustin bilinear transform [17], the discrete equivalent of $G_{PR}(s)$ in *z*-domain can be written as

$$G_{PR}(z) = k_p \frac{a_z z^2 + b_z z + c_z}{A_z z^2 + B_z z + C_z} \qquad (9)$$

where

$a_z = 4 + T_s^2 w_0^2 + 4T_s \xi w_0 + 4T_s \xi k_r w_0$, $b_z = 2T_s^2 w_0^2 - 8$,

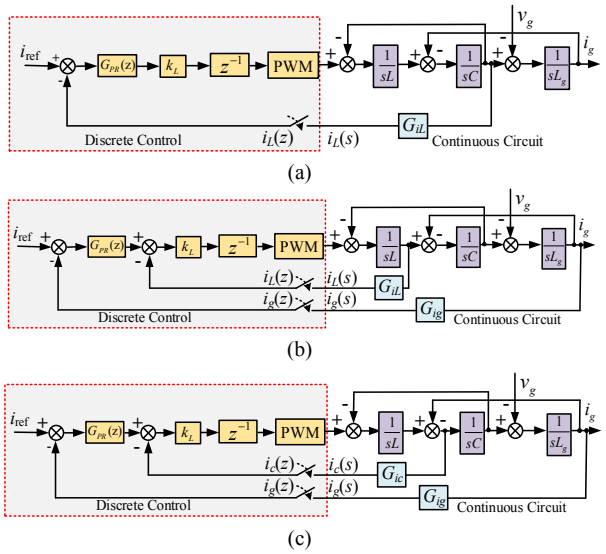

(a)

(b)

(c)

Fig. 4. The z-domain block diagrams of the inverters. (a) The i_L feedback control. (b) The i_L plus i_g feedback control. (c) The i_c plus i_g feedback control

$c_z = 4 + T_s^2 w_0^2 - 4T_s \xi w_0 - 4T_s \xi k_r w_0$, $A_z = T_s^2 w_0^2 + 4\xi T_s w_0 + 4$

$B_z = 2T_s^2 w_0^2 - 8$, $C_z = T_s^2 w_0^2 - 4\xi T_s w_0 + 4$.

The sample and hold circuit in control system lead to one sample delay z^{-1}. The transfer function (2), (3) and (4) describing *LCL* can be discretized includes the effect of the PWM with zero-order hold (ZOH) method [18] .

A. *Influence of Digital Control Delay*

Fig. 5 shows the root locus of the three current feedback control schemes in *z*-plane with the delay time varies from the minimum delay time ($0.5T_s$) to maximum the delay time ($3T_s$), and T_s=50 μs. There are ten poles and nine zeros introduced by the whole system, Z1 is introduced by *LCL*, and P1~P5 are introduced by the delay, P3 is cancelled by Z2.

In Fig.5 (a), with the increasing of T_d, the first cluster of root locus are changing slowly inside the circle, the second cluster of root locus that moving outside the unit circle change a lot. Therefore, when the delay time increases, the system gradually becomes unstable. Besides, comparing with i_L plus i_g and i_c plus i_g feedback system, i_L feedback system is more sensitive to the change of the delay time.

In Fig.5 (b), with the increasing of T_d, P1 (P2) are moving away from the real axis and moving closer to the

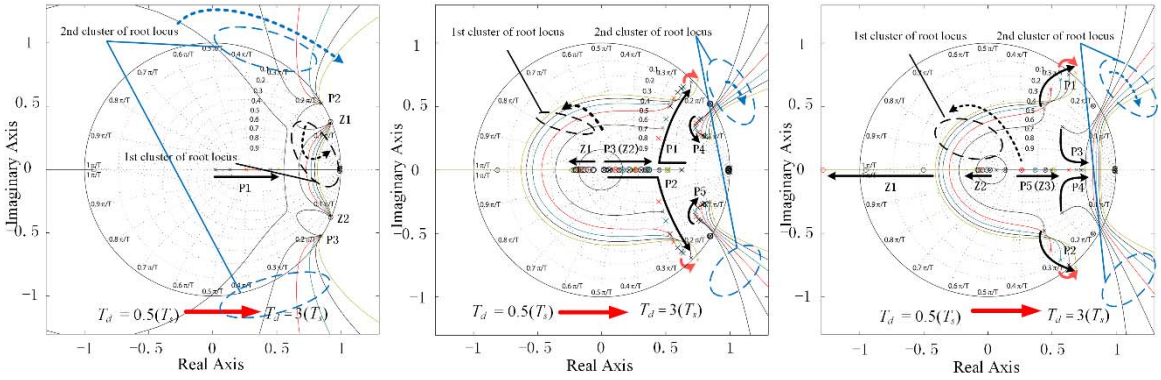

(a) (b) (c)

Fig. 5 . Root loci of three current feedback control schemes considering the variations of the delay time (T_d varies from varies from 0.5 T_s to 3 T_s) in z-plane. (a) The i_L feedback control. (b) The i_L plus i_g feedback control. (c) The i_c plus i_g feedback control

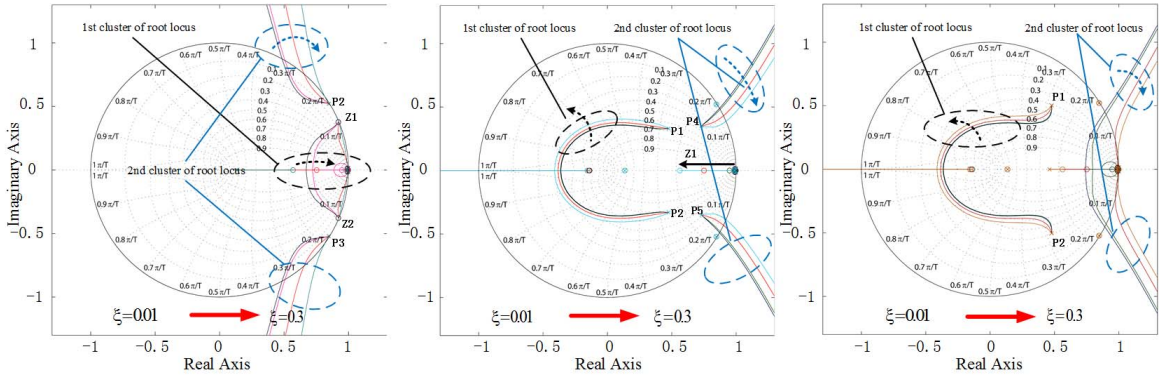

(a) (b) (c)

Fig. 6 . Root loci of three current feedback control schemes considering the variations of the damping factor (ζ varies from 0.01 to 0.3) in z-plane. (a) The i_L feedback control. (b) The i_L plus i_g feedback control. (c) The i_c plus i_g feedback control

unit circle which makes the system inclined to unstable. The second cluster of root locus that start from P4 (P5) and have intersection with the unit circle decide the critical gain of the system. When T_d is less than $2.6T_s$, the critical gain, GM and PM remain almost unchanged. However, when T_d is bigger than 2.6 T_s, the first cluster of root locus begin to have intersection with the unit circle which makes the critical gain, GM and PM reduce dramatically. Thus the stability of the system is affected if T_d is too large.

Fig.5 (c) shows the root locus of i_c plus i_g feedback system when T_d varies. P1~P4 and Z1 are introduced by the delay time, Z2 is introduced by *LCL*. With the increasing of T_d, the first and the second cluster of the root locus are all moving towards outside of the unit circle. The system stability decrease slowly until T_d grows to $2.6T_s$ and the similar result can be obtained from i_L plus i_g feedback control analysis mentioned above.

B. Influence of the damping factor of PR Compensator

The PR compensator can be designed to have a high bandwidth which provides high gain at resonant peaks. System dynamic response can be improved while the stability is also affected. Damping factor ζ is defined as the coefficient of W_0 (W_c=ζW_0=2πf_0ζ) in (1), the influence of ζ varies from 0.01 to 0.3 (W_c changes from 3 to 100 accordingly) on the system root locus is shown in Fig.6.

From Fig.6 (a), with the increasing of ζ, the first and second cluster of root locus are all moving outside the unit circle. The first cluster of root locus begin to across the unit circle when ζ increase to 0.3, thus the system cannot operate in stable state when ζ is too large. In Fig.6 (b), Z1 is introduced by PR and moves towards the circle center when ζ increases. The first cluster of root locus moves towards the unit circle when ζ changes from 0.01 to 0.3, the corresponding critical gain changes from 0.93 to 0.45. When K_p is set to 0.5 and ζ varies from 0.01 to 0.3, the corresponding GM changes from 5.45 dB to 0 dB, PM changes from 115 deg to -17.4 deg. Therefore, when the ζ increases, the system gradually becomes unstable.

In Fig.6 (c), when ζ changes from 0.01 to 0.3, the second cluster of root locus are moving towards the circle. The corresponding critical gain changes from 1.78 to 0.09, and the GM and PM decrease dramatically which indicates that i_c plus i_g feedback system is more sensitive to the change of ζ.

C. Influence of the LCL grid side inductor

The *LCL* filter plays an important role in the grid connected system which achieves higher harmonic attenuation with same (or lower) inductance than *L* filter. The parameters of the inductor, the capacitor and the resistor may change with the variation of the temperate and operation conditions. Therefore, the variation of *LCL* parameters should be taken into account to analyze the system performance. In weak grid case, the wide variation of the grid impedance (L_g) affects the system

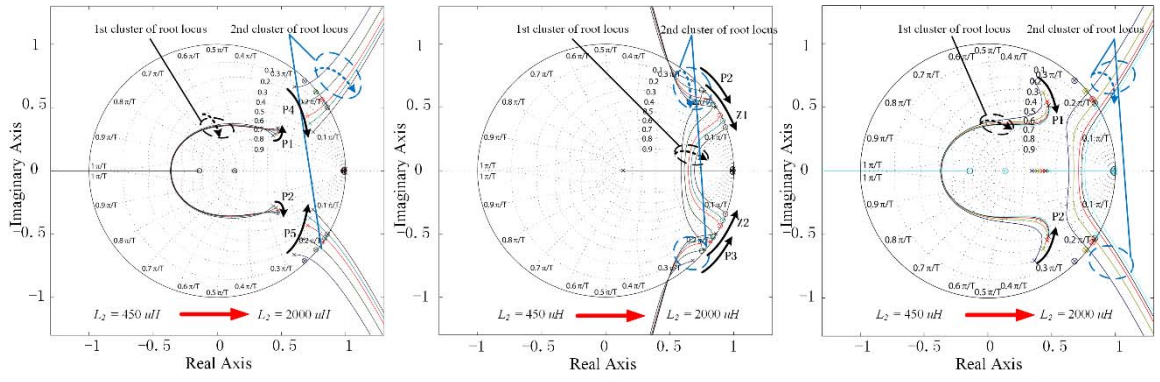

(a) (b) (c)

Fig. 7 . Root loci of three current feedback control system considering the variations of L_2 (L_2 varies from 450μH to 2000μH). (a) The i_L feedback control. (b) The i_L plus i_g feedback control. (c) The i_c plus i_g feedback control

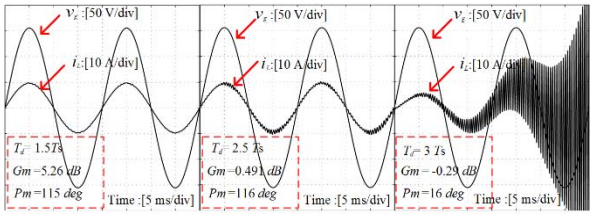

(a) (b) (c)

Fig. 8 . Simulated waveforms of the i_L feedback control when the delay time T_d varies. (a) $T_d = 1.5\ T_s$. (b) $T_d = 2.5\ T_s$. (c) $T_d = 3\ T_s$

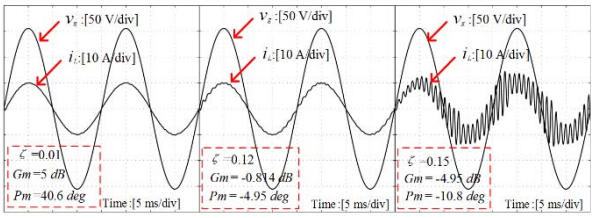

(a) (b) (c)

Fig. 9. Simulated waveforms of the i_c plus i_g feedback control system when ζ varies. (a) ζ=0.01. (b) ζ=0.12. (c) ζ=0.15.

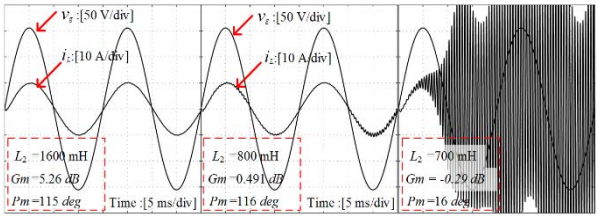

(a) (b) (c)

Fig. 10. Simulated waveforms of the i_L feedback control system when grid side inductor L_2 varies. (a) L_2 =400 mH. (b) L_2 =450 mH. (c) L_2 =1000 mH.

stability significantly. Therefore, the influence of the *LCL* inverter side inductor L_2 is used here to testify the system control stability. The influence of the grid side inductor (L_2) varies from 450μH to 2000μH on the root locus is shown in Fig.7.

In Fig.7 (a), with the increasing of L_2, the first cluster of root locus remains basically unchanged. The second cluster of root locus which start from the poles (P4 and P5) move towards the direction of the arrow. The corresponding critical gain and GM increases gradually thus the system stability is improved, and the PM is affected only when the value of L_2 is lower than 800uH.

As can be seen from Fig.7 (b). P2 (P3) and Z1 (Z2) move towards the same direction while the intersections between the second cluster of root locus and unit circle only change a little. When L_2 varies from 450μH to 2000μH, the corresponding critical gain, GM and PM remain basically unchanged. Which indicate that the variation of L_2 has little effect on the system stability when the i_L plus i_g feedback control scheme are applied.

Fig.7 (c) shows the root locus of i_c plus i_g feedback control scheme when L_2 changes. Compared with Fig.7 (b), it can be seen that the variation tendency of their second cluster root locus are quite similar. The critical gain, PM and GM increases with the increasing of L_2, so the system stability is improved.

D. Summary

When different kinds of feedback control schemes are applied, the converter parameters variation may have different effects on the system stability. When the system delay time increases, the stability of i_L plus i_g and i_c plus i_g feedback system increases slowly. However, once the value of T_d is greater than $2.6T_s$, the corresponding GM and PM decrease dramatically and the system becomes unstable. While the stability of i_L feedback system decrease monotonically when T_d increases. Therefore, in practical application, the delay time should be kept small to ensure the system stability.

When ζ increases, the stability of all three feedback system decreases while i_L plus i_g feedback system have higher stable margin to operate. Therefore, when the system speed respond is ensured, ζ should be kept lower than 0.1. The grid impedance (L_g) can be assumed to be a fraction of the *LCL* converter side inductor L_2, and the proper increase of L_2 can improve the system stability.

IV. Simulation Results

In this paper, three particular simulation waveforms are presented to validate the analysis. Using the parameters listed in Table I, Fig.8 shows the simulation results of the i_L feedback control system when delay time varies. When T_d= 1.5 T_s, the GM=7.85 dB and PM=22.5 deg, thus the system is perfectly stable. When the delay time grows to 2.5 T_s and steps over the stability boundaries, it can be observed that the small-scale oscillations appear on the grid current i_g, and the system is critically stable. When T_d grows to 3 T_s, the system becomes unstable.

Then, Fig.9 shows the simulated waveforms of i_c plus i_g feedback control system when the damping factor ζ varies. From Fig.6 (c), it can be inferred that the stability of the system decreases when ζ increases. In Fig.9, when ζ=0.01, the system bandwidth is suitable, the corresponding GM=5 dB and PM=40.6 deg, so the grid current waveform is sinusoidal. When ζ=0.12, the system is critically stable, and the large-scale oscillations appear on the i_g. When ζ is higher than 0.15, the system becomes unstable.

The simulation results when i_L are used for feedback is shown in Fig. 10. With the increasing of the grid side conductor L_2, the system becomes more stable. When L_2 decreases from 1600 mH to 800 mH, the GM decreases while the PM stay almost unchanged. When L_2 reduces to 700 mH, the corresponding GM drop dramatically below 0 dB so the system becomes unstable.

V. CONCLUSION

In this paper, the digitally controlled grid-connected inverters with the inverter current, the inverter current plus grid current and the capacitor current plus grid current feedback control system have been studied. The impact of the delay time, parameters of the PR compensator and *LCL*-filter on the system stability of three feedback control system are analyzed and compared systematically. The discrete z-domain models are derived which allows direct design of the digital controllers in z-domain model. The results shows that the single-loop converter current feedback control scheme has good dynamic performance when the damping resistor is needed. Dual-loop current feedback control scheme shows better system stability but the dynamic response is also affected. The simulation results are in good agreement with the stability analysis in the *z*-domain models.

REFERENCES

[1] A. Reznik, M. G. Simoes, A. Al-Durra, and S. M. Muyeen, "LCL Filter Design and Performance Analysis for Grid-Interconnected Systems," IEEE Trans. Ind. Appl., vol. 50, pp. 1225-1232, Mar-Apr 2014.

[2] R. Peña-Alzola, M. Liserre, F. Blaabjerg, R. Sebastián, J. Dannehl, and F. W. Fuchs, "Analysis of the Passive Damping Losses in LCL-Filter-Based Grid Converters," Power Electronics, IEEE Transactions on, vol. 28, pp. 2642-2646, 2013.

[3] L. Weiwei, R. Xinbo, P. Donghua, and W. Xuehua, "Full-Feedforward Schemes of Grid Voltages for a Three-Phase LCL-Type Grid-Connected Inverter," Industrial Electronics, IEEE Transactions on, vol. 60, pp. 2237-2250, 2013.

[4] J. Yaoqin, Z. Jiqian, and F. Xiaowei, "Direct Grid Current Control of LCL-Filtered Grid-Connected Inverter Mitigating Grid Voltage Disturbance," IEEE Trans. Power Electron., vol. 29, pp. 1532-1541, 2014.

[5] S. Guoqiao, Z. Xuancai, Z. Jun, and X. Dehong, "A New Feedback Method for PR Current Control of LCL-Filter-Based Grid-Connected Inverter," IEEE Trans. Ind. Electron., vol. 57, pp. 2033-2041, 2010.

[6] H. Azani, A. Massoud, L. Benbrahim, B. W. Williams, and D. Holiday, "An LCL filter-based grid-interfaced three-phase voltage source inverter: Performance evaluation and stability anaylsis," in Power Electronics, Machines and Drives (PEMD 2014), 7th IET International Conference on, 2014, pp. 1-6.

[7] B. Li, W. Yao, L. Hang, and L. M. Tolbert, "Robust proportional resonant regulator for grid-connected voltage source inverter (VSI) using direct pole placement design method," Iet Power Electronics, vol. 5, pp. 1367-1373, 2012.

[8] T. Yi, L. Poh Chiang, W. Peng, C. Fook Hoong, and G. Feng, "Exploring Inherent Damping Characteristic of LCL-Filters for Three-Phase Grid-Connected Voltage Source Inverters," IEEE Trans. Power Electron., vol. 27, pp. 1433-1443, 2012.

[9] M. Castilla, J. Miret, J. Matas, L. G. de Vicua, and J. M. Guerrero, "Linear Current Control Scheme With Series Resonant Harmonic Compensator for Single-Phase Grid-Connected Photovoltaic Inverters," Industrial Electronics, IEEE Transactions on, vol. 55, pp. 2724-2733, 2008.

[10] H. M. El-Deeb, A. Elserougi, A. S. Abdel-Khalik, S. Ahmed, and A. M. Massoud, "Performance assessment of single and dual loops discrete PR controllers with LCL filter for inverter-based distributed generation," in Power Electronics, Electrical Drives, Automation and Motion (SPEEDAM), 2014 International Symposium on, 2014, pp. 500-505.

[11] L. Poh Chiang and D. G. Holmes, "Analysis of multiloop control strategies for LC/CL/LCL-filtered voltage-source and current-source inverters," Industry Applications, IEEE Transactions on, vol. 41, pp. 644-654, 2005.

[12] D. H. Pan, X. B. Ruan, C. L. Bao, W. W. Li, and X. H. Wang, "Capacitor-Current-Feedback Active Damping With Reduced Computation Delay for Improving Robustness of LCL-Type Grid-Connected Inverter," IEEE Trans. Power Electron., vol. 29, pp. 3414-3427, Jul 2014.

[13] X. T. Zhang, J. W. Spencer, and J. M. Guerrero, "Small-Signal Modeling of Digitally Controlled Grid-Connected Inverters With LCL Filters," IEEE Trans. Ind. Electron., vol. 60, pp. 3752-3765, Sep 2013.

[14] A. G. Yepes, A. Vidal, J. Malvar, O. Lopez, and J. Doval-Gandoy, "Tuning Method Aimed at Optimized Settling Time and Overshoot for Synchronous Proportional-Integral Current Control in Electric Machines," Power Electronics, IEEE Transactions on, vol. 29, pp. 3041-3054, 2014.

[15] L. Fei, Z. Yan, D. Shanxu, Y. Jinjun, L. Bangyin, and L. Fangrui, "Parameter Design of a Two-Current-Loop Controller Used in a Grid-Connected Inverter System With LCL Filter," Industrial Electronics, IEEE Transactions on, vol. 56, pp. 4483-4491, 2009.

[16] Y. Jinjun, D. Shanxu, and L. Bangyin, "Stability Analysis of Grid-Connected Inverter With LCL Filter Adopting a Digital Single-Loop Controller With Inherent Damping Characteristic," IEEE Trans. Ind. Inform., vol. 9, pp. 1104-1112, 2013.

[17] A. G. Yepes, F. D. Freijedo, J. Doval-Gandoy, Lo, x, O. pez, et al., "Effects of Discretization Methods on the Performance of Resonant Controllers," Power Electronics, IEEE Transactions on, vol. 25, pp. 1692-1712, 2010.

[18] A. Vidal, F. D. Freijedo, A. G. Yepes, P. Fernandez-Comesana, J. Malvar, O. Lopez, et al., "Assessment and Optimization of the Transient Response of Proportional-Resonant Current Controllers for Distributed Power Generation Systems," IEEE Trans. Ind. Electron., vol. 60, pp. 1367-1383, Apr 2013.